

Preparation of Al₂O₃/Au nano-laminated composite coatings and their oxidation resistance on stainless steel

GAO Jun-guo¹, LU Feng¹, TANG Zhi-hui¹, WANG Chang-liang¹, HE Ye-dong²

1. Metal Corrosion and Surface Protection Laboratory,
Beijing Institute of Aeronautical Materials, Beijing 100095, China;
2. Beijing Key Laboratory for Corrosion, Erosion and Surface Technology,
University of Science and Technology Beijing, Beijing 100083, China

Received 9 July 2012; accepted 8 August 2012

Abstract: Al₂O₃/Au nano-laminated composite coatings were prepared by means of magnetron sputtering. The coating was compact and comprised of nano-laminated Al₂O₃ and Au layers. High temperature cyclic oxidation test was employed to investigate the oxidation resistance of the composite coatings. The results revealed that the applied Al₂O₃/Au nano-laminated composite coatings improved the oxidation and spallation resistance of the stainless steel substrate significantly. The mechanism accounting for oxidation resistance was related with the suppression of inward oxygen diffusion and selective oxidation of Cr in the substrate. The mechanism accounting for spallation resistance was attributed to the relaxation of thermal stress by the nano-laminated structure.

Key words: Al₂O₃/Au composite coatings; magnetron sputtering; oxidation resistance; spallation resistance

1 Introduction

High-temperature oxidation failure of alloys is extensively concerned in many fields, such as aeronautics and astronautics, petrochemical industry, power generation and waste incineration. High-temperature oxidation will bring about not only huge economic losses but also destructive service safety problems [1]. The pursuit of alloys providing both good mechanical properties and excellent oxidation resistance seems to be a shortcut for solving such problems. However, both of the requirements sometimes can not be achieved by alloy development itself. Therefore, a composite system including alloy substrates and surface coatings in which good mechanical properties can be achieved by alloy development and excellent high-temperature oxidation resistance by surface coating or surface modification has been developed as an approach to meet both of the requirements. Researches showed that this strategy works well in many industrial applications. To date, ceramic coatings [2,3] and metallic coatings [4,5] are the two basic and important high-temperature protective coatings. For ceramic

coatings, Al₂O₃ is widely used owing to its extremely low oxygen diffusion coefficient [6]. Nevertheless, the thermal expansion mismatch between Al₂O₃ and alloy substrate becomes one of the most important factors restricting its further development. And for the metallic coatings, noble metals such as Au and Pt are considered ideal high-temperature coating materials due to their excellent thermodynamic stability and low oxygen diffusion rate [7]. However, with the service of the coating, the inter-diffusion between the coating and alloy substrate is prone to causing the failure of the coating. Besides that, the high cost of noble metals is also one of the concerned problems.

Recently, multilayered composite materials have drawn more and more attention in various applications due to their unique performance compared with monophasic materials. Layered composites have been proposed as an excellent design to enhance the strength reliability of components as well as to improve their fracture toughness by means of energy release mechanisms, such as crack deflection or crack bifurcation [8,9]. It was found that the laminated system exhibits an apparent fracture toughness which is twice higher than the value determined for the monolithic

materials [10]. HO and SUO [11] found that there was a critical thickness for the constrained brittle layer bonded between tougher substrates under residual and applied stresses during the investigation of tunneling cracks (such a crack initiates from an equi-axed flaw, confined by the substrates, tunneling in the brittle layer), and below the thickness, no tunneling cracks occurred regardless of the size of original cracks. Therefore, the decrease of layer thickness in laminated system is very beneficial to suppressing crack extension.

In this work, Al₂O₃/Au nano-laminated composite coatings were prepared by magnetron sputtering. The oxidation resistance of such coatings on stainless steel was investigated and the mechanisms accounting for their excellent high-temperature oxidation and spallation resistance were also discussed.

2 Experimental

2.1 Preparation of Al₂O₃/Au nano-laminated composite coatings

The Al₂O₃/Au nano-laminated composite coatings were prepared using an opposite-targets magnetron sputtering (MS) system (Model TUS-800MP, Technol. Ltd., Co., Beijing). 1Cr18Ni9Ti stainless steel with the cut size of 15 mm×10 mm×2 mm was used as the substrate. The specimens were precisely polished ($R_a=0.03 \mu\text{m}$) and ultrasonically cleaned in ethanol before sputtering. The specimens were fixed on a rotating specimen holder in order to ensure that all surfaces of the substrate can be sputtered uniformly. The Al₂O₃ layer was deposited by radio-frequency MS using an α -Al₂O₃ ceramic target and the Au layer was deposited by direct current MS using an Au target (purity >99.99%). The layers of Al₂O₃ and Au were deposited alternately onto the substrate with the order of Al₂O₃-Au-Al₂O₃-Au-Al₂O₃. The operating parameters during sputtering the Al₂O₃/Au nano-laminated composite coatings are shown in Table 1. The as-prepared coatings were subsequently vacuum heat pretreated at 1000 °C for 6 h to promote Al₂O₃ transforming from amorphous to crystalline.

Table 1 Operating parameters of magnetron sputtering

Operating parameter	Operating value
Base pressure/Pa	5×10^{-4}
Working pressure/Pa	0.5–1.0
Distance between target and specimen/cm	7
Heating temperature/°C	150
Rotational speed of specimen/(r·min ⁻¹)	10
Power of direct current sputtering/W	90
Power of radio-frequency sputtering/W	70

2.2 High-temperature cyclic oxidation test

The high-temperature cyclic oxidation test which was one type of the accelerated life tests was employed to investigate the oxidation and spallation resistance of the Al₂O₃/Au nano-laminated composite coatings on stainless steel under oxidation condition. The test was performed in a horizontal furnace at 900 °C for 100 h. After a certain oxidation period of 10 h, the samples were taken out and rapidly cooled to room temperature in 30 min as a cycle. The mass gain (specimen + crucible) and spallation mass (crucible without the specimen) were respectively weighed at each interval using an electronic balance with an accuracy of 10^{-4} g. After the measurement, the samples were put back to the furnace immediately. The test providing 10 times of thermal cycles can also evaluate the thermal shock resistance and mechanical properties of the as-prepared coatings.

2.3 Characterization

The morphology and elements analysis of the Al₂O₃/Au nano-laminated composite coatings before and after high-temperature oxidation test were characterized by a high-resolution field emission scanning electron microscope (FE-SEM, ZEISS SUPRA 55) equipped with an energy-dispersive X-ray spectroscope (EDX). Phases of the specimens after oxidation were identified by X-ray diffractometer (XRD, Rigaku D/max-PB 2400) with a graphite monochromatized Cu K α radiation flux at a scanning rate of 0.02 (°)/s in the 2θ range of 10°–100°.

3 Results

3.1 Morphologies of as-prepared Al₂O₃/Au nano-laminated composite coatings

The surface and cross-sectional morphologies of the as-prepared Al₂O₃/Au nano-laminated composite coatings are shown in Fig. 1. It could be seen that after sputtering and heat treatment, the surface of the nano-laminated coating was composed of uniform nano-particles. According to the sputtering sequence of deposition layers, 5 layers with the order of Al₂O₃-Au-Al₂O₃-Au-Al₂O₃ from surface to interface were observed from cross-sectional morphology. The thickness of the Al₂O₃ and Au layers were 60–80 nm and 20 nm, respectively. And different layers of the nano-laminated coating were combined compactly.

3.2 High-temperature cyclic oxidation kinetics

Figure 2 presents the cyclic oxidation kinetic curves of the blank and coating specimens at 900 °C in air for 100 h. With respect to the mass gain and scale spallation, it could be found from the curves that the blank sample exhibited a very fast rate of oxidation as well as severe scale spallation during cyclic oxidation. During the

oxidation test, the oxidation scale of the blank sample would spall off at each cycle, which induced that the mass gain and spallation mass increased with time prolonging continuously. On the contrast, the coating specimen exhibited an extremely low mass gain and scale spallation mass. It can be seen that the amount of mass gain and spallation mass decreased by two and

three orders of magnitude, respectively, due to the sputtering of $\text{Al}_2\text{O}_3/\text{Au}$ nano-laminated composite coatings.

3.3 Characterization of specimens after high-temperature cyclic oxidation

Figure 3 shows the surface and cross-section images

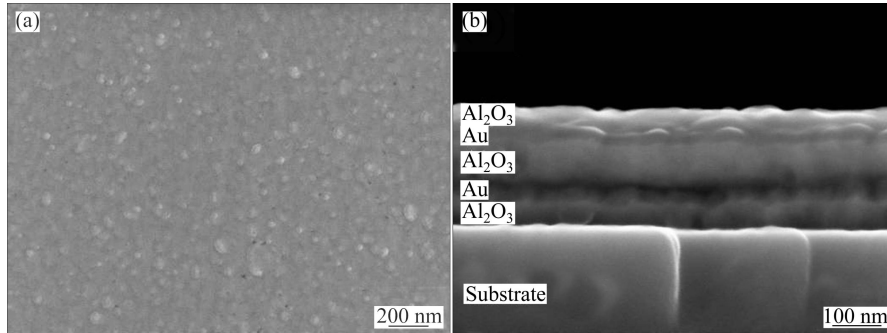


Fig. 1 Surface (a) and cross-section (b) morphologies of as-prepared $\text{Al}_2\text{O}_3/\text{Au}$ nano-laminated composite coatings

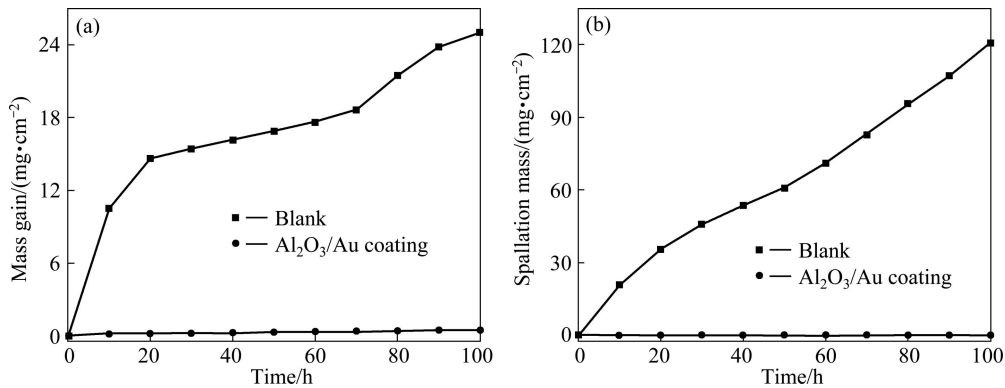


Fig. 2 Cyclic oxidation kinetic curves of blank and coating specimens at 900 °C for 100 h: (a) Mass gain vs time; (b) Spallation mass vs time

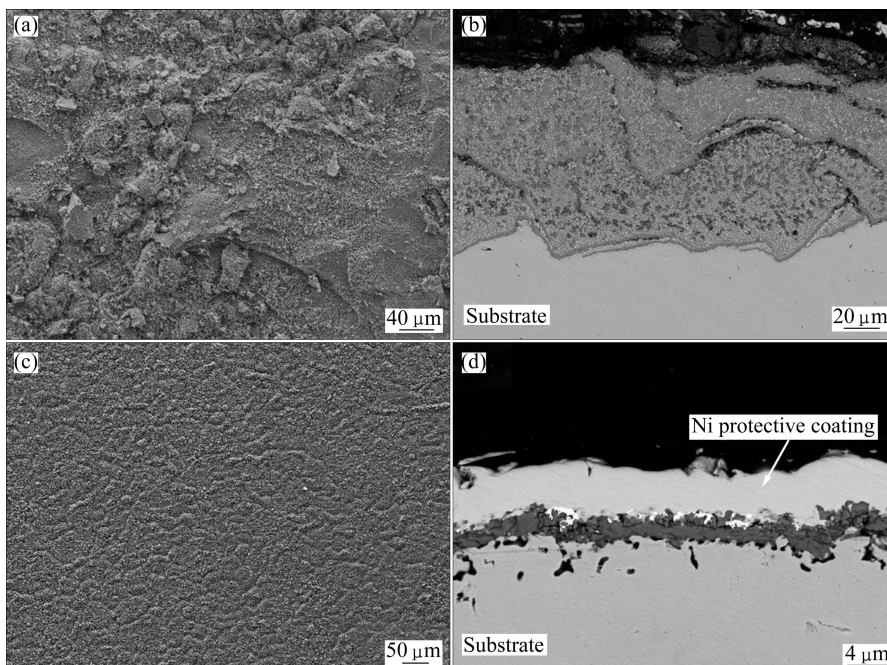


Fig. 3 Surface (a, c) and cross-section (b, d) images of different specimens after cyclic oxidation at 900 °C for 100 h: (a, b) Blank sample; (c, d) Coating specimen

of different specimens after cyclic oxidation at 900 °C for 100 h. The surface of the blank sample became very rough after oxidation and the spallation trail of oxidation scale can also be found on the surface. However, the surface of the coating specimen was comparatively smooth and no crack or spallation occurred on the surface. By comparing the cross-section morphologies as shown in Figs. 3(b) and (d), it can be seen that the oxidation scale of the blank sample was relatively thick and uneven. In contrast, the oxidation scale of the coating specimen was comparatively thin and uniform. But the morphology of the $\text{Al}_2\text{O}_3/\text{Au}$ nano-laminated composite coating was difficult to be found due to the inward diffusion of oxygen and the outward diffusion of metallic elements during oxidation.

The cross-sectional elements distribution of the blank sample after cyclic oxidation at 900 °C for 100 h is shown in Fig. 4. It can be seen obviously that the oxidation scale of the blank sample was composed of both chromium oxide and ferric oxide. And cracks can

be found on the top of the oxidation scale. Compared with the blank sample, the cross-sectional elements distribution of the coating specimen after oxidation (Fig. 5) exhibited that the oxidation scale of the coating specimen consisted of only chromium oxide and no ferric oxide. The chromium oxide scale was compact and continuous. However, the distribution of elements Al and Au was not detected due to the small thickness of the $\text{Al}_2\text{O}_3/\text{Au}$ nano-laminated composite coating and the diffusion of elements during oxidation.

Figure 6 shows the XRD spectra of different specimens after cyclic oxidation at 900 °C for 100 h. It can be seen that the oxidation scale of the blank sample was composed of Fe_2O_3 and the mixture of Fe_2O_3 and Cr_2O_3 ($(\text{Fe}_{0.6}\text{Cr}_{0.4})_2\text{O}_3$), which was consistent with the elements distribution in Fig. 4. With respect to the coating specimen, strong peaks of the stainless steel substrate were identified due to the small thickness of the coating and oxide, which was close to the penetration depth of X-ray (about several microns). Besides that,

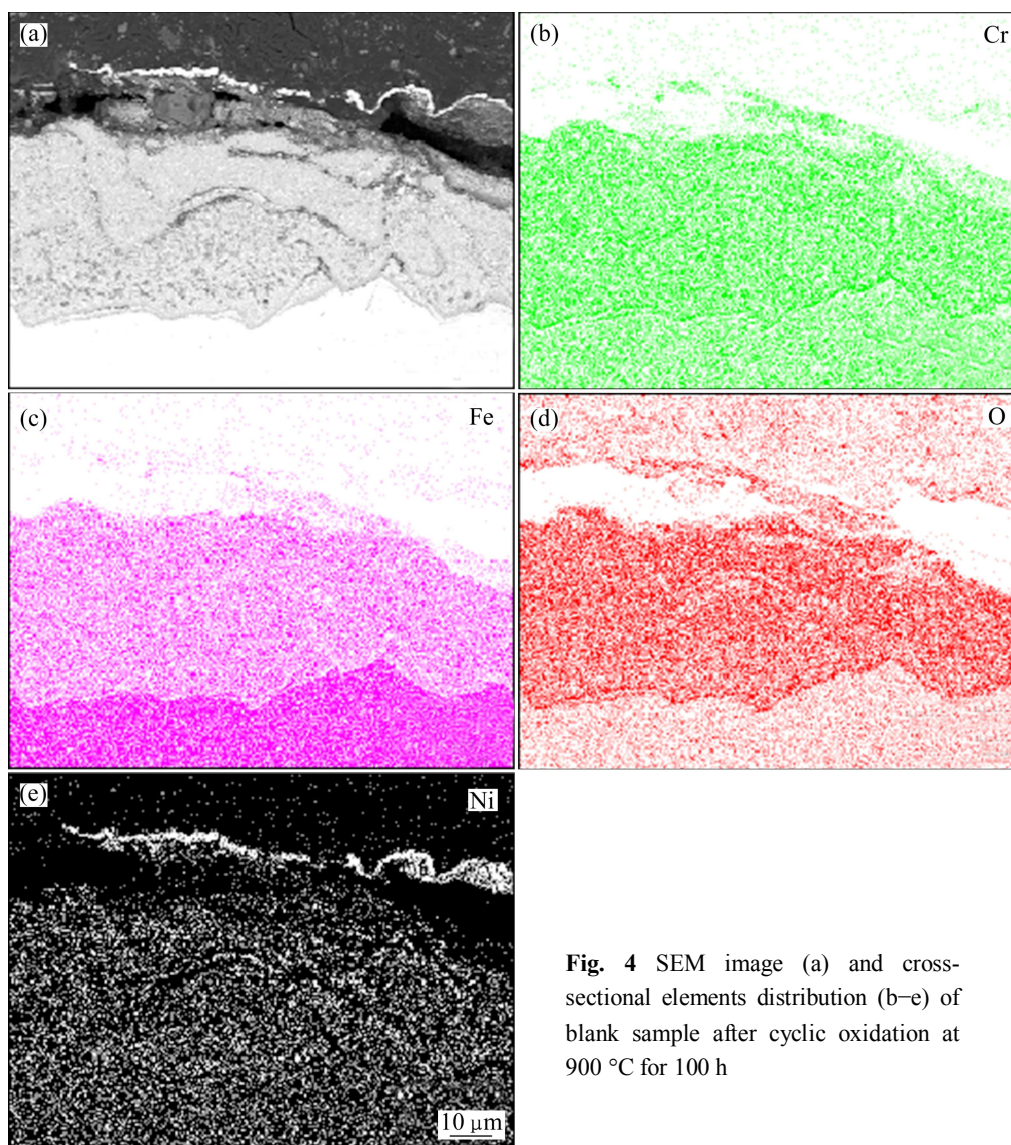


Fig. 4 SEM image (a) and cross-sectional elements distribution (b–e) of blank sample after cyclic oxidation at 900 °C for 100 h

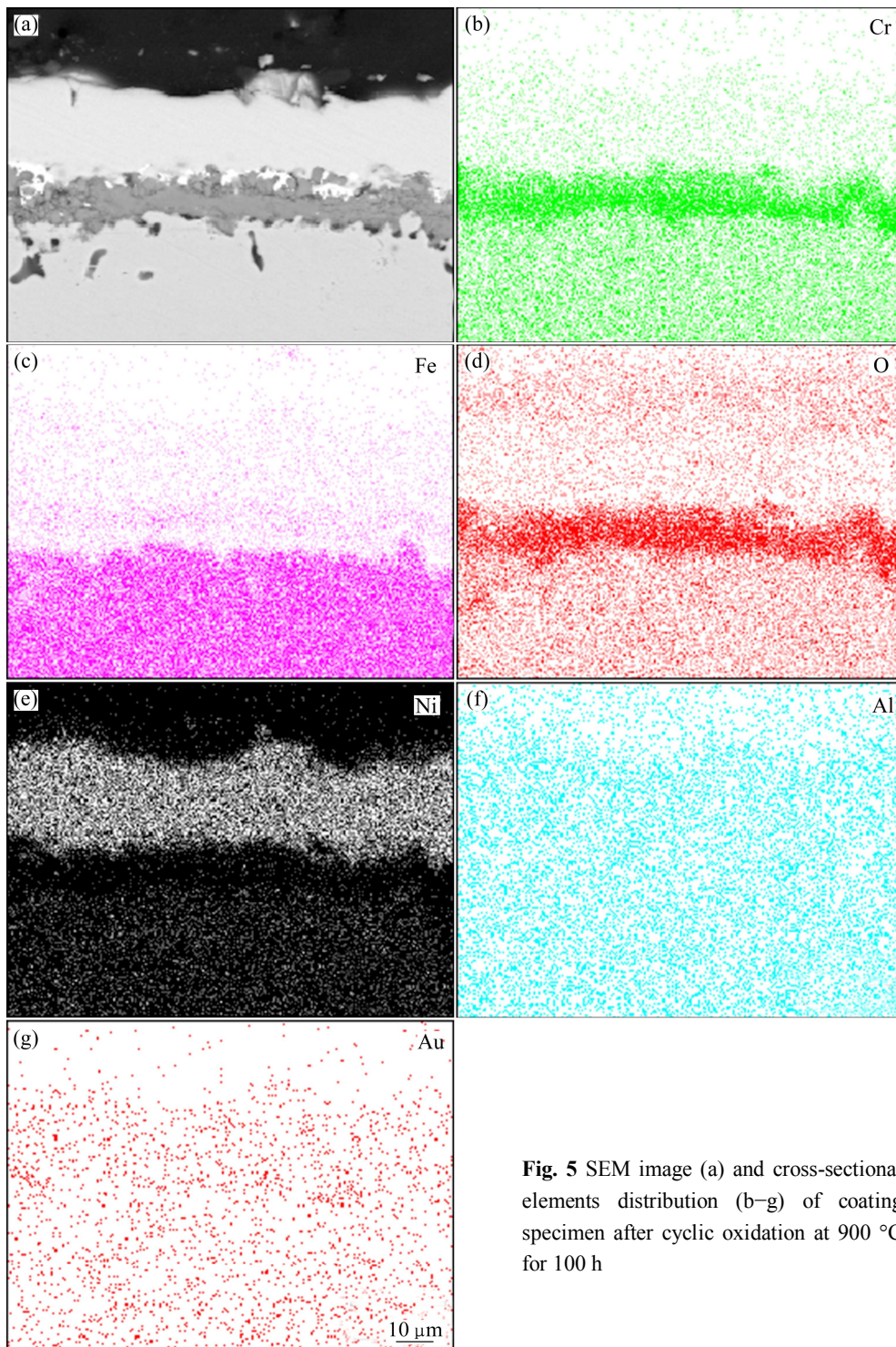


Fig. 5 SEM image (a) and cross-sectional elements distribution (b–g) of coating specimen after cyclic oxidation at 900 °C for 100 h

peaks of α -Al₂O₃ and Cr₂O₃, which came from the coating and oxidation scale, respectively, were also identified. No peaks of Au were detected due to its little content in the composite coating.

4 Discussion

The oxidation resistance of stainless steel substrate

under cyclic oxidation at 900 °C was significantly improved by the applied Al₂O₃/Au nano-laminated composite coatings. As shown in Fig. 7, the mechanisms accounting for such superior performance can be explained from two aspects as follows.

On one hand, the Al₂O₃/Au nano-laminated composite coating has a positive influence on suppressing the inward diffusion of oxygen and promoting

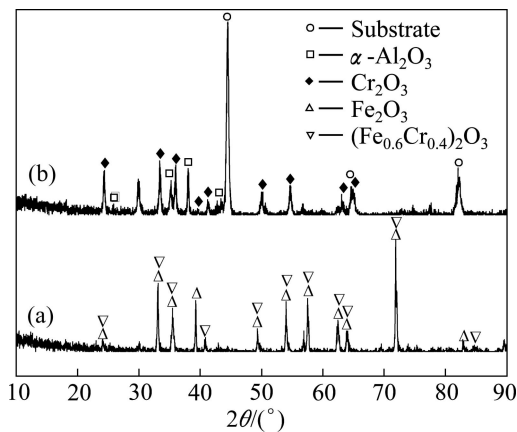


Fig. 6 XRD spectra of specimens after cyclic oxidation at 900 °C for 100 h: (a) Blank sample; (b) Coating specimen

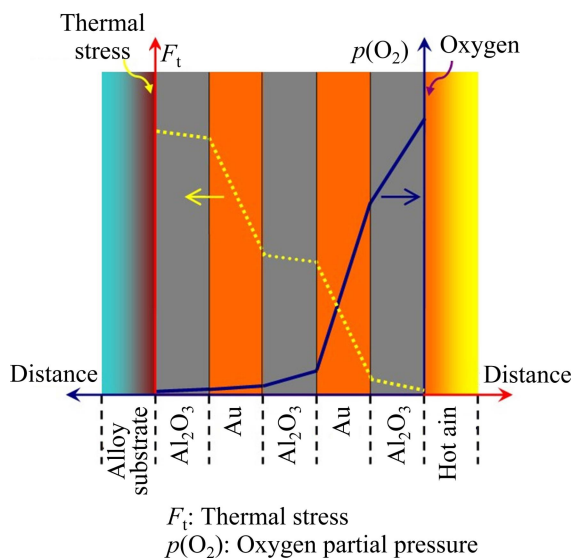


Fig. 7 Model of oxygen diffusion and thermal stress release in $\text{Al}_2\text{O}_3/\text{Au}$ nano-laminated composite coatings

selective oxidation of the substrate. It is well known that the dense and defect-free $\alpha\text{-Al}_2\text{O}_3$ layer is considered to be one of the most effective diffusion barriers in protecting alloy substrate from oxidation owing to its extremely low oxygen diffusion coefficient [12]. Besides that, the noble metal Au which theoretically does not oxidize under high temperature is also an excellent oxygen diffusion barrier [13]. Therefore, as the oxygen diffusion model shown in Fig. 7, the outside oxygen partial pressure can be decreased quickly to an extremely low level at the coating/substrate interface due to the applying of the coating. As a result, the parabolic rate constant (k_p) of the alloy substrate oxidation will be decreased greatly due to the low oxygen partial pressure at the coating/substrate interface. According to WAGNER's theory on the selective oxidation of alloys [14], the critical concentration of B solute in an A–B alloy to form a selective BO external scale can be

expressed as:

$$N_B = \frac{V}{Z_B M_O} \left(\frac{\pi k_p}{D} \right)^{\frac{1}{2}}$$

where k_p is the parabolic rate constant, V is the molar volume of alloy, Z_B is the valence of B, M_O is the relative atom mass of oxygen, and D is the diffusivity of B in the alloy. As mentioned above, the applied $\text{Al}_2\text{O}_3/\text{Au}$ nano-laminated composite coating will lead to the decrease of k_p greatly. With the decrease of k_p , the critical concentration of Cr in the substrate will subsequently descend, which will promote the selective oxidation of Cr to form Cr_2O_3 (see Fig. 3(d) and Fig. 5). And the dense and continuous Cr_2O_3 layer will also play an important role in protecting the substrate from further oxidation.

On the other hand, the unique design of $\text{Al}_2\text{O}_3/\text{Au}$ nano-laminated structures will bring about excellent mechanical properties which can protect the coating from failure effectively. For the Al_2O_3 layers, nano structures were observed as shown in Fig. 1(a). Superplasticity was demonstrated in fine-grained ceramics and ceramic composites including yttria-stabilized tetragonal zirconia [15] and alumina [16]. Large ductilities were recorded for the above ceramics. The fine structure of Al_2O_3 layers may give rise to superplasticity which is helpful for relaxing thermal stress generated during thermal cycling. And for the Au layers, their capability of plastic deformation will also play an important role in relaxing thermal stress. Therefore, the nano-laminated structures of the $\text{Al}_2\text{O}_3/\text{Au}$ composite coating are apt to release the high temperature thermal stress as the model shown in Fig. 7 and thus improve the spallation resistance of the coating significantly.

In conclusion, the excellent oxidation and spallation resistance of the $\text{Al}_2\text{O}_3/\text{Au}$ nano-laminated composite coatings on stainless steel substrate are attributed to the synergetic effect of the unique constituent and structure design of the coating.

5 Conclusions

1) $\text{Al}_2\text{O}_3/\text{Au}$ nano-laminated composite coatings were successfully prepared by means of magnetron sputtering. The coating was laminated by the order of $\text{Al}_2\text{O}_3\text{-Au-Al}_2\text{O}_3\text{-Au-Al}_2\text{O}_3$. And the thickness of the Al_2O_3 and Au layers was 60–80 nm and 20 nm, respectively.

2) The $\text{Al}_2\text{O}_3/\text{Au}$ composite coatings exhibited excellent oxidation and spallation resistance on stainless steel substrate. Compared with the blank substrate, the value of mass gain and spallation mass decreased by two or three orders of magnitude, respectively.

3) The mechanism accounting for oxidation resistance was related with the suppression of inward oxygen diffusion and selective oxidation of Cr in the substrate. The mechanism accounting for spallation resistance was attributed to the relaxation of thermal stress by the nano-laminated structure.

References

- [1] MA X, HE Y, WANG D, ZHANG J. Superior high-temperature oxidation resistance of a novel (Al₂O₃-Y₂O₃)/Pt laminated coating [J]. Appl Sur Sci, 2012, 258: 4733–4740.
- [2] LAKIZA S M, LOPATO L M. Stable and metastable phase relations in the system alumina-zirconia-yttria [J]. J Am Ceram Soc, 1997, 80: 893–902.
- [3] MEDRAJ M, HAMMOND R, PARVEZ M A, DREW R A L, THOMPSON W T. High temperature neutron diffraction study of the Al₂O₃-Y₂O₃ system [J]. J Eur Ceram Soc, 2006, 26: 3515–3524.
- [4] YANG X, PENG X, WANG F. Hot corrosion of a novel electrodeposited Ni-6Cr-7Al nanocomposite under molten (0.9Na,0.1K)₂SO₄ at 900 °C [J]. Scripta Mater, 2007, 56: 891–894.
- [5] DEODESHMUKH V, MU N, LI B, GLEESON B. Hot corrosion and oxidation behavior of a novel Pt+Hf-modified γ'-Ni₃Al + γ-Ni-based coating [J]. Surf Coat Technol, 2006, 201: 3836–3840.
- [6] HOSODA H, MIYAZAKI S, HANADA S. Potential of IrAl base alloys as ultrahigh-temperature smart coatings [J]. Intermetallics, 2000, 8: 1081–1090.
- [7] THONSTAD J. Anodic overvoltage on platinum in cryolite-alumina melts [J]. Electrochim Acta, 1968, 13: 449–456.
- [8] SÁNCHEZ-HERENCIA A J, JAMES L, LANGE F F. Bifurcation in alumina plates produced by a phase transformation in central, alumina/zirconia thin layers [J]. J Eur Cer Soc, 2000, 20: 1297–1300.
- [9] OECHSNER M, HILLMAN C, LANGE F F. Crack bifurcation in laminar ceramic composites [J]. J Am Ceram Soc, 1996, 79: 1834–1838.
- [10] BERMEJO R, TORRES Y, BAUDÍN C, SÁNCHEZ-HERENCIA A J, PASCUAL J, ANGLADA M, LLANES L. Threshold strength evaluation on an Al₂O₃-ZrO₂ multilayered system [J]. J Eur Ceram Soc, 2007, 27: 1443–1448.
- [11] HO S, SUO Z. Tunneling cracks in constrained layers [J]. J Appl Mech-T ASME, 1993, 60: 890–894.
- [12] HEUER A H. Oxygen and aluminum diffusion in α-Al₂O₃: How much do we really understand [J]. J Eur Ceram Soc, 2008, 28: 1495–1507.
- [13] MERKER J, LUPTON D, TÖPFER M, KNAKE H. High temperature mechanical properties of the platinum group metals [J]. Platinum Met Rev, 2001, 45: 74–82.
- [14] WAGNER C. Theoretical analysis of the diffusion processes determining the oxidation rates of alloys [J]. J Electrochem Soc, 1952, 99: 369–380.
- [15] TEKELI S, DAVIES T J. Improvement of tensile ductility in 3 mol-percent yttria-stabilized tetragonal zirconia (3Y-TZP) by prestraining [J]. J Mater Sci, 1998, 33: 1145–1149.
- [16] CHEN I W, XUE L A. Development of superplastic structural ceramics [J]. J Am Ceram Soc, 1990, 73: 2585–2609.

Au/Al₂O₃ 层状复合纳米涂层的制备及其抗氧化性能

高俊国¹, 陆峰¹, 汤智慧¹, 王长亮¹, 何业东²

1. 北京航空材料研究院 金属腐蚀与防护研究室, 北京 100095;
2. 北京科技大学 北京市腐蚀、磨蚀与表面技术重点实验室, 北京 100083

摘要: 采用磁控溅射法成功制备 Al₂O₃/Au 层状复合纳米涂层, 所制备的涂层结构致密且由 Al₂O₃ 层和 Au 层交替组成。采用高温循环氧化实验对复合涂层在不锈钢基体上的高温抗氧化性能进行分析评价。结果表明: Al₂O₃/Au 层状复合纳米涂层极大地改善不锈钢基体的抗氧化和抗剥落性能。其抗氧化机理与涂层能够有效地抑制氧向合金基体的扩散并促进不锈钢基体中 Cr 元素的选择性氧化有关; 抗剥落机理可归因于复合涂层中的 Au 层和纳米结构的 Al₂O₃ 层能够有效地松弛高温热循环过程中产生的热应力, 从而提高涂层的抗剥落性能。

关键词: Al₂O₃/Au 复合涂层; 磁控溅射; 抗氧化性能; 抗剥落性能

(Edited by YUAN Sai-qian)